

Scale Dependence of Squark and Gluino Production Cross Sections

Edmond L. Berger^a, Michael Klasen^a, and Tim Tait^{a,b}

^a*High Energy Physics Division, Argonne National Laboratory*

Argonne, Illinois 60439

^b*Michigan State University, East Lansing, Michigan 48824*

(September 12, 2018)

Abstract

We investigate the choice of the renormalization and factorization scales for the production of squarks and gluinos at the Fermilab Tevatron collider as a function of the produced sparticle masses. We determine a scale to be used in leading-order perturbative QCD calculations *optimized* such that the normalization of the next-to-leading order cross section is reproduced. Use of this optimal scale permits at least a partial implementation of next-to-leading order contributions in leading order Monte Carlo simulations. We provide next-to-leading order predictions of the production cross sections for pairs of supersymmetric particles at the hadronic center-of-mass energy 2 TeV.

12.38.Bx, 12.60.Jv, 13.85.Fb

I. INTRODUCTION

The possibility of supersymmetry (SUSY) at the electroweak scale and the ongoing search for the Standard Model (SM) Higgs boson constitute two major and related aspects of the motivation for the Tevatron upgrade currently under construction at Fermilab. The increase in the center-of-mass energy to 2 TeV and the luminosity to an expected 2 fb^{-1} , together with detector improvements, should permit discovery or exclusion of supersymmetric partners of the standard model particles up to much higher masses than at present. A hadron collider like the Tevatron is particularly well suited for the production of strongly interacting sparticles, squarks and gluinos, among which the light stop eigenstate is expected to have the lowest mass value.

Experimental searches for supersymmetry rely heavily on Monte Carlo simulations of cross sections and event topologies. Two Monte Carlo generators in common use include SUSY processes; they are ISAJET [1] and SPYTHIA [2,3]. Production cross sections may also be computed analytically from fixed-order quantum chromodynamics (QCD) perturbation theory. Calculations that include contributions through next-to-leading order (NLO) in QCD have been performed for the production of squarks and gluinos [4], stops [5], and more recently of sleptons [6] and neutralinos [7]. The cross sections can be calculated as functions of the sparticle masses and thus do not depend on a particular SUSY breaking mechanism.

Both the Monte Carlo approach and the fixed order approach have different advantages and limitations. Next-to-leading order perturbative calculations depend on very few parameters, e.g., the renormalization and factorization scales, and the dependence of the production cross sections on these parameters is reduced significantly in NLO with respect to leading order (LO). Therefore, the normalization of the cross section can be calculated quite reliably if one includes the NLO contributions. On the other hand, the existing next-to-leading order calculations provide predictions only for fully inclusive quantities, e.g., a differential cross section for production of a squark or a gluino, after integration over all other particles and variables in the final state. In addition, they do not include sparticle decays. This approach

does not allow for event shape studies nor for experimental selections on missing energy or other variables associated with the produced sparticles or their decay products that are crucial if one wants to enhance the SUSY signal in the face of substantial backgrounds from Standard Model processes.

The natural strength of Monte Carlo simulations consists in the fact that they generate event configurations that resemble those observed in experimental detectors. Through their parton showers, these generators include, in the collinear approximation, contributions from all orders of perturbation theory. In addition, they incorporate phenomenological hadronization models, a simulation of particle decays, the possibility to implement experimental cuts, and event analysis tools. However, the hard-scattering matrix elements in these generators are accurate only to leading order in QCD, and, owing to the rather complex nature of infra-red singularity cancellation in higher orders of perturbation theory, it remains a difficult challenge to incorporate the full structure of NLO contributions successfully in Monte Carlo simulations. The limitation to leading-order hard-scattering matrix elements leads to large uncertainties in the normalization of the cross section. The parton shower and hadronization models rely on tunable parameters, another source of uncertainties.

The aim of this paper is to improve the accuracy of the normalization of cross sections computed through Monte Carlo simulations. We introduce some aspects of the reliability and normalization of next-to-leading order calculations while preserving the flexibility and event shape versatility of Monte Carlo simulations. This goal can be approached in at least two ways, with different secondary consequences. The first method is simply to multiply the leading order cross section computed in the Monte Carlo simulation by an overall K -factor. The second, the method we adopt and investigate, is to select a renormalization and factorization (hard) scale in the Monte Carlo LO calculation such that, with this choice of hard scale, the normalization of the Monte Carlo LO calculation agrees with that of the NLO perturbative calculation. The answer one obtains in both approaches will in general depend on which partonic subprocess one is considering and on the kinematics. However, only a change in the hard scale will affect both the hard matrix element *and* the initial-state and

final-state parton shower radiation. A rescaling of the cross section by an overall K -factor will have no bearing on the parton shower radiation. A reduction in the hard scale leads generally to less evolution and less QCD radiation, and vice-versa, in the initial- and final-state showering. A change of the hard scale will be reflected in the normalization of the cross section as well as in the event shape. We suggest that the approach we adopt is a more consistent combination of next-to-leading order and parton shower effects.

The outline of this paper is as follows: In Section 2, we briefly review the calculation of next-to-leading order hadronic cross sections for squark and for gluino production. In Section 3, we discuss the hard scale dependence at leading order and at next-to-leading order. Our main results are presented in Section 4. There we show the dependence of the optimal scale choices on the produced sparticle masses. A summary is given in Section 5.

II. SQUARK AND GLUINO PRODUCTION AT NEXT-TO-LEADING ORDER

We consider the pair production of strongly interacting supersymmetric particles in proton-antiproton scattering. The total cross section can be calculated as a function of the hadronic center-of-mass energy $\sqrt{s_H}$ and the produced sparticle mass \tilde{m} through the factorization theorem

$$\sigma_{p\bar{p}}^{\text{total}}(s_H, \tilde{m}^2) = \sum_{a,b=q,\bar{q},g} \int dx_a dx_b f_p^a(x_a, M^2) f_{\bar{p}}^b(x_b, M^2) \hat{\sigma}_{ab}(x_a x_b s_H, \tilde{m}^2; M^2). \quad (1)$$

We set $\sqrt{s_H} = 2$ TeV for Tevatron Run II conditions.

The parton densities $f_{p,\bar{p}}^{a,b}$ depend on the longitudinal light-cone momentum fractions $x_{a,b}$ of the quarks and gluons in the proton and antiproton, respectively, as well as on the factorization scale M . We treat the gluon and the five light quark flavors as massless and use the CTEQ4M parametrization [8] throughout this paper. For the top quark, we assume a mass of 175 GeV and neglect its contribution to the parton densities.

The partonic cross section $\hat{\sigma}$ depends on the partonic center-of-mass energy $x_a x_b s_H$, on the produced sparticle mass \tilde{m} , and on the factorization scale M . It can be calculated in fixed order perturbative QCD by an expansion in the strong coupling strength

$$\hat{\sigma}_{ab}(x_a x_b s_H, \tilde{m}^2; M^2) = \alpha_s^2(\mu^2) \hat{\sigma}_{ab}^{\text{tree}} + \alpha_s^3(\mu^2) \hat{\sigma}_{ab}^{\text{loop}}(\mu^2) + \alpha_s^3(\mu^2) \hat{\sigma}_{ab}^{\text{real}}(M^2) + \mathcal{O}(\alpha_s^4). \quad (2)$$

The renormalization scale is denoted μ . At leading order, the only dependence on μ arises in the strong coupling strength α_s since only tree-level $2 \rightarrow 2$ processes are taken into account.

The partonic subprocesses that contribute at this stage are:

$$q + \bar{q}, g + g \longrightarrow \tilde{q} + \bar{\tilde{q}}, \quad (3)$$

$$q + q \longrightarrow \tilde{q} + \tilde{q}, \quad (4)$$

$$q + \bar{q}, g + g \longrightarrow \tilde{g} + \tilde{g}, \quad (5)$$

$$q + g \longrightarrow \tilde{q} + \tilde{g}, \quad (6)$$

$$q + \bar{q}, g + g \longrightarrow \tilde{t}_1 + \bar{\tilde{t}}_1. \quad (7)$$

At next-to-leading order, both virtual loop diagrams and real emission diagrams contribute. The real emission contributions are integrated over the soft and collinear regions of the additional third parton. Through the renormalization procedure, logarithmic terms arising in the virtual diagrams partly cancel the leading order renormalization scale dependence. The collinear singularities in the real emission diagrams are absorbed into the parton densities, introducing logarithmic dependence on the factorization scale. Therefore, we also expect a reduced factorization scale dependence. A detailed presentation of the next-to-leading order calculation can be found in Refs. [4,5].

In this paper, all sparticle masses are set to

$$\tilde{m} = [m_{\tilde{q}}; m_{\tilde{g}}; (m_{\tilde{q}} + m_{\tilde{g}})/2] = 250 \text{ GeV}, \quad (8)$$

if not stated otherwise, with the exception of the light stop mass $m_{\tilde{t}_1} = 153 \text{ GeV}$. The strong Yukawa coupling between the top quark, its supersymmetric partner, and the Higgs field leads to large mixing of the left- and right-handed stops and to a $\tilde{t}_1(\tilde{t}_2)$ mass that is expected to lie below (above) the other squark masses. Therefore, we treat the light stop \tilde{t}_1 here separately from the other squarks and ignore the heavy stop \tilde{t}_2 . The particular mass value of $m_{\tilde{t}_1} = 153 \text{ GeV}$ results from a minimal supergravity-inspired solution of the

renormalization group equations with input values $m_0 = m_{1/2} = 100$ GeV, $A_0 = 300$ GeV, $\tan\beta = 1.75$ and $\mu > 0$. The mixing angle is found to be $\sin(2\tilde{\theta}) = -0.99$. This is the only place where an assumption of a specific SUSY breaking mechanism is made. The squark and gluino mass values are chosen in such a way that they are above experimental exclusion limits but within reach of Run II at the Tevatron.

In Figs. 1-5 we present the next-to-leading order values for the production cross sections for all strong SUSY channels as a function of sparticle mass at 2 TeV. Also provided are the leading order values. In obtaining the numerical results presented in this paper, we use a modified version of the PROSPINO code [9], with the FORTRAN altered to run on the VAX/VMS platform. We have verified that our results agree with those in Refs. [4] and [5] when we select the same center-of-mass energy and other parameters. For our results, we set the common hard scale $\mu = M$ equal to $\mu = \tilde{m}$ in both the leading and the next-to-leading order calculations. For our next-to-leading order results, we use the hard matrix elements through next-to-leading order, parton densities evolved with next-to-leading order Altarelli-Parisi kernels, and the two-loop expression for the strong coupling strength $\alpha_s(\mu)$. For the leading order results, the only change we make is to use the leading order hard matrix element. In this way, we are able to identify how much of the increase in cross section at next-to-leading order is due to the hard scattering matrix element. For the leading order results, one could also employ leading order definitions of all three components. It could be argued that our procedure might not be consistent philosophically. However, the difference is of next-to-leading order so that both determinations of the leading order cross section are equally consistent up to terms of $\mathcal{O}(\alpha_s^3)$. Of more importance to us is to study the effect of the next-to-leading order matrix element and not the well-known universal effects of the higher order terms in the parton densities or the coupling constant. In addition, the extraction of leading order parton densities is more uncertain, and some packages of parton densities (e.g., MRS [10]) do not include a leading order option.

In the case of SUSY particle production, the next-to-leading order contributions are known to increase the production cross sections by 50 % and more. For the various channels

we consider, the increase can be seen explicitly in Figs. 1-5. For example, in Fig. 1 we plot the total cross section for squark-antisquark production as a function of the squark mass. The next-to-leading order cross section (full curve) lies above the leading order cross section (dashed curve) by 59 %. This increase translates into a shift in the lower limit of the produced squark mass of 19 GeV. The cross sections for gluino pair production (Fig. 3) and the associated production of squarks and gluinos of equal mass (Fig. 4) are of similar magnitude, whereas the squark pair production (Fig. 2) and stop-antistop production (Fig. 5) cross sections are smaller by about an order of magnitude [4,5].

III. SCALE DEPENDENCE AT LEADING ORDER AND AT NEXT-TO-LEADING ORDER

In this section, we study the dependence of the leading and next-to-leading order cross sections for squark and gluino production on the renormalization and factorization scales. The cross section is expected to depend principally on the produced sparticle mass \tilde{m} . Therefore, we set the renormalization and factorization scales equal, $\mu = M \equiv Q$, and calculate our results as a function of Q/\tilde{m} .

Figure 6 presents the total cross section for squark-antisquark production as a function of the common renormalization and factorization scale Q . The squark mass has been fixed at $m_{\tilde{q}} = 250$ GeV. It is common to estimate the theoretical uncertainty by examining the variation of the calculated cross section over an interval of $Q/m_{\tilde{q}} = [0.5; 2.0]$. The strong scale dependence of 63 % for the leading order cross section (dashed curve) is reduced to 31 % (i.e., ± 15.5 % about a central value) for the next-to-leading order cross section (full curve), smaller but still considerable. For $Q = m_{\tilde{q}}$, the next-to-leading order cross section can be obtained from the leading order cross section if the latter is multiplied by a K -factor of 1.59. The same increase is obtained if a scale $Q = 0.41 m_{\tilde{q}}$ is used in the calculation of the leading order cross section.

In Figs. 7 and 8, we show the hard scale dependence of the cross sections for gluino pair

production and associated production of a squark and gluino. In these plots, as in those for squark-squark and stop-antistop production, a scale variation of about $\pm 18\%$ about a central value is observed in the values of the next-to-leading order cross sections, similar to that in Fig. 6.

In the literature, two scale choices are sometimes preferred. We advocate neither of these, but we mention them to distinguish them from the phenomenologically-based range of scales that we suggest in Sec. IV be used in leading order calculations. The Principle of Minimal Sensitivity (PMS) scale is specified by [11]

$$\frac{d\sigma_{\text{NLO}}}{dQ}(Q_{\text{PMS}}) = 0. \quad (9)$$

It has the advantage that in the neighborhood of Q_{PMS} , a variation in the scale results in no change of the next-to-leading order (NLO) cross section. The Principle of Fastest Convergence (PFC) scale is defined by [12]

$$\sigma_{\text{NLO}}(Q_{\text{PFC}}) = \sigma_{\text{LO}}(Q_{\text{PFC}}). \quad (10)$$

Its virtue is that the NLO correction is absent, and the perturbative series seems to converge rapidly. Although next-to-next-to-leading (NNLO) order terms might well spoil both, the prescriptions provide some guidance until these NNLO corrections are calculated.

The Principle of Minimal Sensitivity and the Principle of Fastest Convergence have been shown to be consistent with each other up to NNLO terms [13]. However, the Principle of Fastest Convergence answer depends on whether the leading order (LO) cross section is defined with LO expressions throughout or in the hard matrix element only. Due to the larger value of α_s in the one-loop approximation, the first approach leads to a larger LO cross section. This alternative usually moves the PFC scale away from the PMS scale.

In Fig. 7 we present the total cross section for gluino pair production as a function of the common renormalization and factorization scale Q . The gluino mass has been fixed at $m_{\tilde{g}} = 250$ GeV. The scales preferred by the Principle of Minimal Sensitivity (PMS), $Q = 0.35 m_{\tilde{g}}$, and the Principle of Fastest Convergence (PFC), $Q = 0.36 m_{\tilde{g}}$, are close

to each other if the leading order choice is restricted to the hard matrix element only. If the parton densities and α_s are calculated in leading order as well, the PFC scale shifts to $Q = 0.37 m_{\tilde{g}}$.

IV. OPTIMAL SCALE CHOICES

The aim of this section is to determine optimal scale choices to be used in leading order calculations of squark and gluino production at the Tevatron. If implemented in leading order Monte Carlo generators such as ISAJET [1] or SPYTHIA [2,3], these optimal scales will reproduce the size of the NLO cross section:

$$\sigma_{\text{LO}}(Q_{\text{LO}}/\tilde{m}) = \sigma_{\text{NLO}}(Q_{\text{NLO}}/\tilde{m}). \quad (11)$$

To illustrate our definition of optimal scale choices, we show in Fig. 8 the total cross section for associated squark and gluino production as a function of the common renormalization and factorization scale Q . The squark and gluino masses are fixed at $m_{\tilde{q}} = m_{\tilde{g}} = 250$ GeV. The NLO cross section depends on the scale choice. Correspondingly, there is not a unique choice of scale in LO that will reproduce the NLO value of the cross section but, rather, a range of values that will reproduce the band of NLO values. As is done commonly, we define the theoretical uncertainty in the NLO value by the spread associated with three different scale choices $2Q_{\text{NLO}}/(m_{\tilde{q}} + m_{\tilde{g}}) = [0.5; 1.0; 2.0]$. The corresponding cross sections are reproduced in leading order by the somewhat narrower band of scales, $2Q_{\text{LO}}/(m_{\tilde{q}} + m_{\tilde{g}}) = [0.35; 0.475; 0.6]$.

The cross sections for the hadroproduction of squarks and gluinos depend strongly on the produced sparticle mass. We expect some sparticle mass dependence also in the optimal scale choices that reproduce the size of the next-to-leading order cross sections at leading order. This dependence is demonstrated in Fig. 9, where we plot the optimal scale choices for associated squark and gluino production as a function of the average squark and gluino mass $(m_{\tilde{q}} + m_{\tilde{g}})/2$. For the central (full) curve, the NLO scale is chosen equal to the average

squark and gluino mass. The dashed and dotted curves define the remaining uncertainty at NLO from a variation of $2Q_{\text{NLO}}/(m_{\bar{q}} + m_{\tilde{g}}) = [0.5; 2.0]$. In this plot, we set $m_{\bar{q}} = m_{\tilde{g}}$.

The three-dimensional Fig. 10 shows the optimal scale choices for the same process as a function of both the squark mass $m_{\bar{q}}$ and the gluino mass $m_{\tilde{g}}$. The dependence on $m_{\bar{q}}$ and $m_{\tilde{g}}$ separately is much weaker than along the diagonal that represents the average squark and gluino mass $(m_{\bar{q}} + m_{\tilde{g}})/2$. This average would seem to be a preferable physical scale for the process instead of either of the two produced sparticle masses.

The squark mass dependence of the optimal scale choice for squark-antisquark and squark pair production is plotted in Figs. 11 and 12. For these processes, as well as for the associated production of squarks and gluinos, the dependence on parameters other than the produced sparticle mass is negligible. On the other hand, in the case of gluino pair production the optimal scale shows a large sensitivity in the region where $m_{\tilde{g}} = m_{\bar{q}}$. The strong sensitivity is displayed in Figs. 13 and 14, where we set $m_{\bar{q}} = 250$ and 450 GeV, respectively. The sensitivity arises from the fact that the LO Born cross section decreases with increasing squark mass in the region of $m_{\tilde{g}} \sim m_{\bar{q}}$, whereas the NLO virtual and soft contributions increase. A strong variation of the relative size of the two contributions results in that region. Figure 15 shows the optimal scale choice for the same channel as a function of both the gluino mass $m_{\tilde{g}}$ and the squark mass $m_{\bar{q}}$. The large sensitivity is apparent along the diagonal where $m_{\tilde{g}} = m_{\bar{q}}$.

The results for stop-antistop production are shown in Fig. 16 as a function of the stop mass $m_{\tilde{t}_1}$. In this case, dependence on the light squark and gluino masses is negligible again.

For ease of implementation in Monte Carlo generators, we summarize our results in Table I. For the five different production channels we provide optimal values of the scale to be used in LO calculations in order to reproduce the values of the NLO cross sections obtained at three different values of the hard scale in the next-to-leading order calculations. It is evident that one cannot adopt a single preferred LO scale for any one of the subprocess nor a single next-to-leading order scale, independent of sparticle mass, unless one is prepared to bias the cross section. The principal variation one sees is due to the dominant dependence of

the cross sections on the produced sparticle mass, and the optimal scale generally decreases with increasing sparticle mass.

V. SUMMARY

In this paper, we present next-to-leading order cross sections for squark and gluino production at a center-of-mass energy of $\sqrt{s_H} = 2$ TeV. The hard scale dependence of the cross section at leading order in perturbative QCD is reduced at NLO but not entirely absent. For three choices of the scale used in the next-to-leading order calculations, we define optimal scales that can be used in leading order Monte Carlo simulations. If these optimal scales are used, the size of the next-to-leading order cross section is reproduced. The values of the optimal scales depend mainly on the produced sparticle mass, with the exception of the case of gluino pair production where sensitivity in the region near $m_{\tilde{g}} = m_{\tilde{q}}$ requires special attention. One may be tempted to use a single scale in all processes and for all masses, but the price is to bias the cross section determination. Our results allow one to select hard scales in LO calculations so that the resulting cross sections will reproduce a range of next-to-leading order cross sections, from optimistic to pessimistic values.

In this paper, cross sections are for inclusive yields, integrated over all transverse momenta and rapidities. In the search for supersymmetric states, a selection on transverse momentum will normally be applied in order to improve the signal to background conditions. Our analysis can also be carried out with similar selections. A tabulation of cross sections for various squark and gluino masses is available upon request.

There is little doubt that the reliability of Monte Carlo codes is an important issue. All current exclusion limits on masses of sparticles are based on Monte Carlo simulations. However, not enough is known about the systematic uncertainties associated with the use of Monte Carlo simulations, especially in view of the fact that signals for sparticles are sought in relatively small corners of phase space. A change in the hard scale from the oft assumed value of Q/\tilde{m} approximately 1.0 to Q/\tilde{m} in the interval 0.2 to 0.6, as we determine, will

change the transverse momentum distributions of sparticles in the final state, making their detection either more or less probable. To find out how much change results, one must compare results obtained from runs of the Monte Carlo codes with the different values of the scale. The change will provide a new measure of the theoretical systematic uncertainty.

ACKNOWLEDGMENTS

Work in the High Energy Physics Division at Argonne National Laboratory is supported by the U.S. Department of Energy, Division of High Energy Physics, Contract W-31-109-ENG-38. We have benefitted from communications with H. Baer, M. Spira, and C. Wagner, and are grateful to M. Spira for providing a copy of his numerical code.

REFERENCES

- [1] F.E. Paige, S.D. Protopopescu, H. Baer, and X. Tata, Brookhaven report BNL-HET-98-18, hep-ph/9804321.
- [2] T. Sjöstrand, Comput. Phys. Commun. **82**, 74 (1994).
- [3] S. Mrenna, Comput. Phys. Commun. **101**,232 (1997).
- [4] W. Beenakker, R. Höpker, M. Spira, and P.M. Zerwas, Nucl. Phys. **B492**, 51 (1997).
- [5] W. Beenakker, M. Krämer, T. Plehn, M. Spira, and P.M. Zerwas, Nucl. Phys. **B515**, 3 (1998).
- [6] H. Baer, B.W. Harris, and M.H. Reno, Phys. Rev. **D57** (1998) 5871.
- [7] W. Beenakker, M. Klasen, M. Krämer, T. Plehn, M. Spira, and P.M. Zerwas, Talks given by M. Krämer and M. Spira at the Workshop on Theory of LHC Processes, CERN, Geneva, Switzerland, February 1998.
- [8] H.L. Lai, J. Huston, S. Kuhlmann, F. Olness, J. Owens, D. Soper, W.K. Tung, and H. Weerts, Phys. Rev. **D55**, 1280 (1997).
- [9] W. Beenakker, R. Höpker, M. Spira, hep-ph/9611232.
- [10] A.D. Martin, R.G. Roberts, W.J. Stirling, and R.S. Thorne, RAL-TR-1998-029, Contribution to the 6th International Workshop on Deep Inelastic Scattering and QCD (DIS 98), Brussels, Belgium, April 1998, hep-ph/9805205.
- [11] P.M. Stevenson, Phys. Lett. **100B**, 61 (1981); Phys. Rev. **D23**, 2916 (1981).
- [12] G. Grunberg, Phys. Lett. **95B**, 70 (1980). Erratum *ibid.* **110B** (1982) 501.
- [13] J. Kubo and S. Sakakibara, Phys. Rev. **D26**, 3656 (1982).

TABLES

Channel	$Q_{\text{NLO}}/\tilde{m} = 0.5$	$Q_{\text{NLO}}/\tilde{m} = 1.0$	$Q_{\text{NLO}}/\tilde{m} = 2.0$
$\tilde{q}\tilde{q}$	0.35 - 0.15	0.45 - 0.25	0.60 - 0.30
$\tilde{q}\tilde{q}$	0.40 - 0.15	0.45 - 0.20	0.60 - 0.20
$\tilde{g}\tilde{g}$	0.45 - 0.15	0.50 - 0.20	0.75 - 0.25
$\tilde{q}\tilde{g}$	0.40 - 0.20	0.50 - 0.35	0.60 - 0.40
$\tilde{t}_1\tilde{t}_1$	0.50 - 0.20	0.60 - 0.35	0.70 - 0.40

TABLE I. Optimal scale choices for the production of squarks and gluinos at the Tevatron Run II for five different production channels and three different choices of the next-to-leading order scale. The variation is due to the dominant dependence of the optimal scale on the produced sparticle mass over the range \tilde{m} from 50 to 850 GeV. The optimal scale generally decreases with increasing sparticle mass.

FIGURES

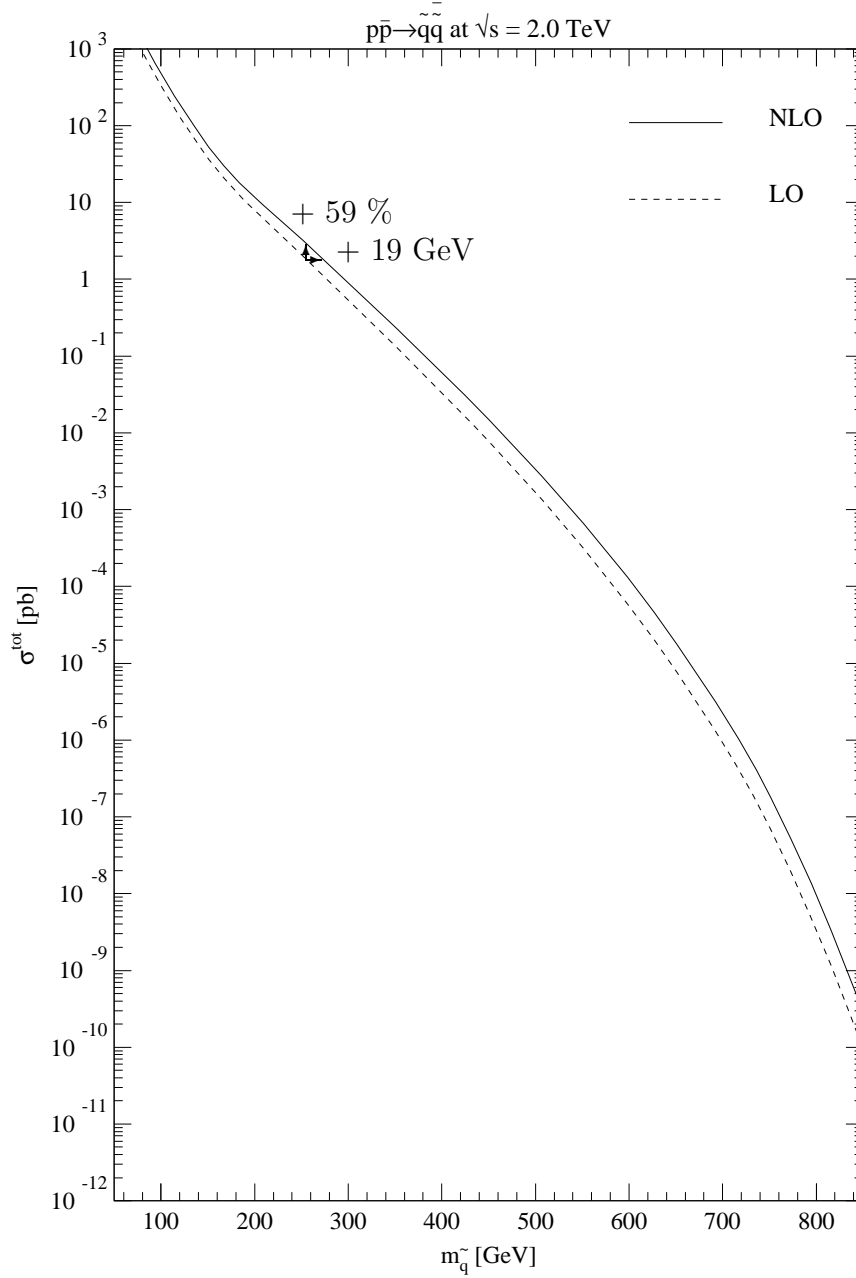


FIG. 1. Total cross section for squark-antisquark production at Run II of the Tevatron as a function of squark mass. The next-to-leading order cross section (full curve) exceeds the leading order cross section (dashed curve) by 59 %. Alternatively, for any measured cross section the corresponding squark mass is shifted by 19 GeV. The gluino mass has been fixed at $m_{\tilde{g}} = 250$ GeV.

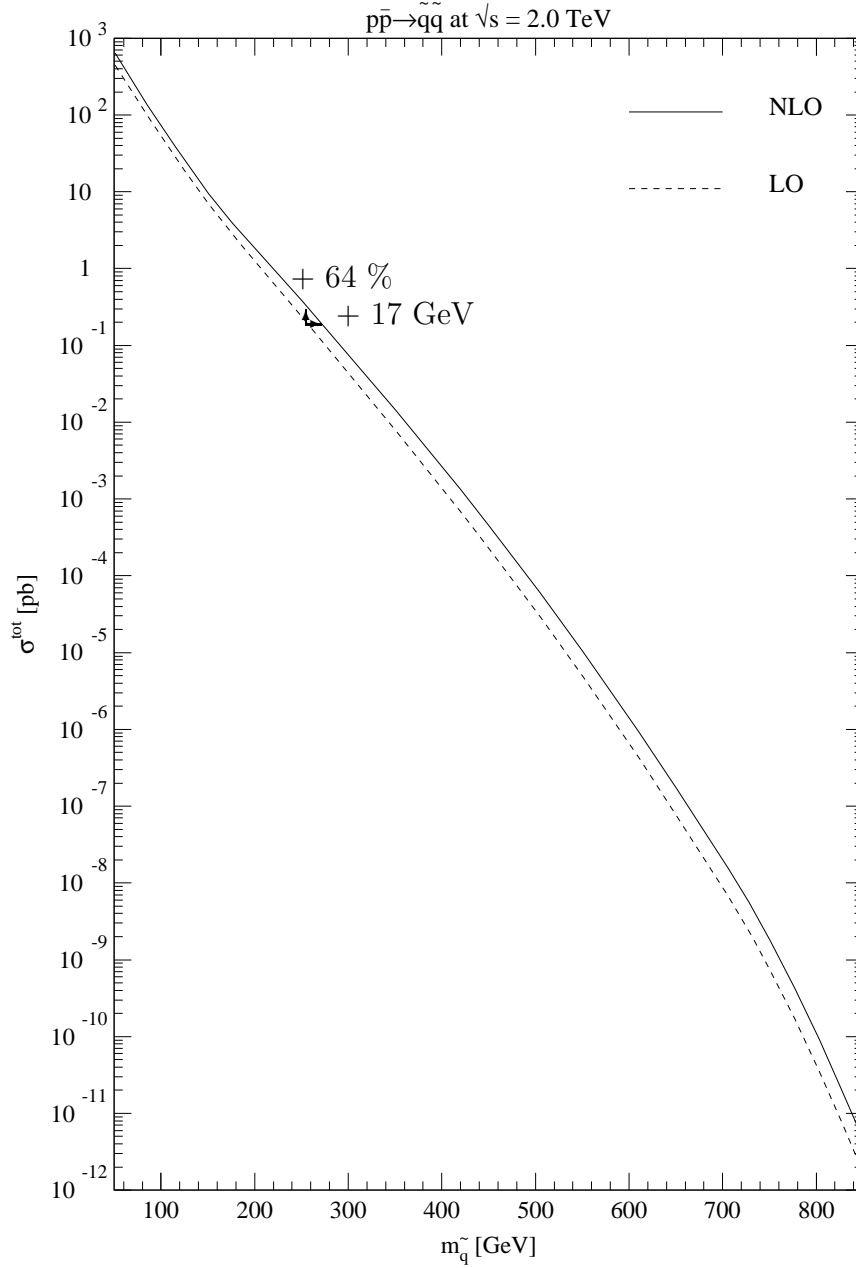


FIG. 2. Total cross section for squark pair production at Run II of the Tevatron as a function of squark mass. The next-to-leading order cross section (full curve) exceeds the leading order cross section (dashed curve) by 64 %. Alternatively, for any measured cross section the corresponding squark mass is shifted by 17 GeV. The gluino mass has been fixed at $m_{\tilde{g}} = 250$ GeV.

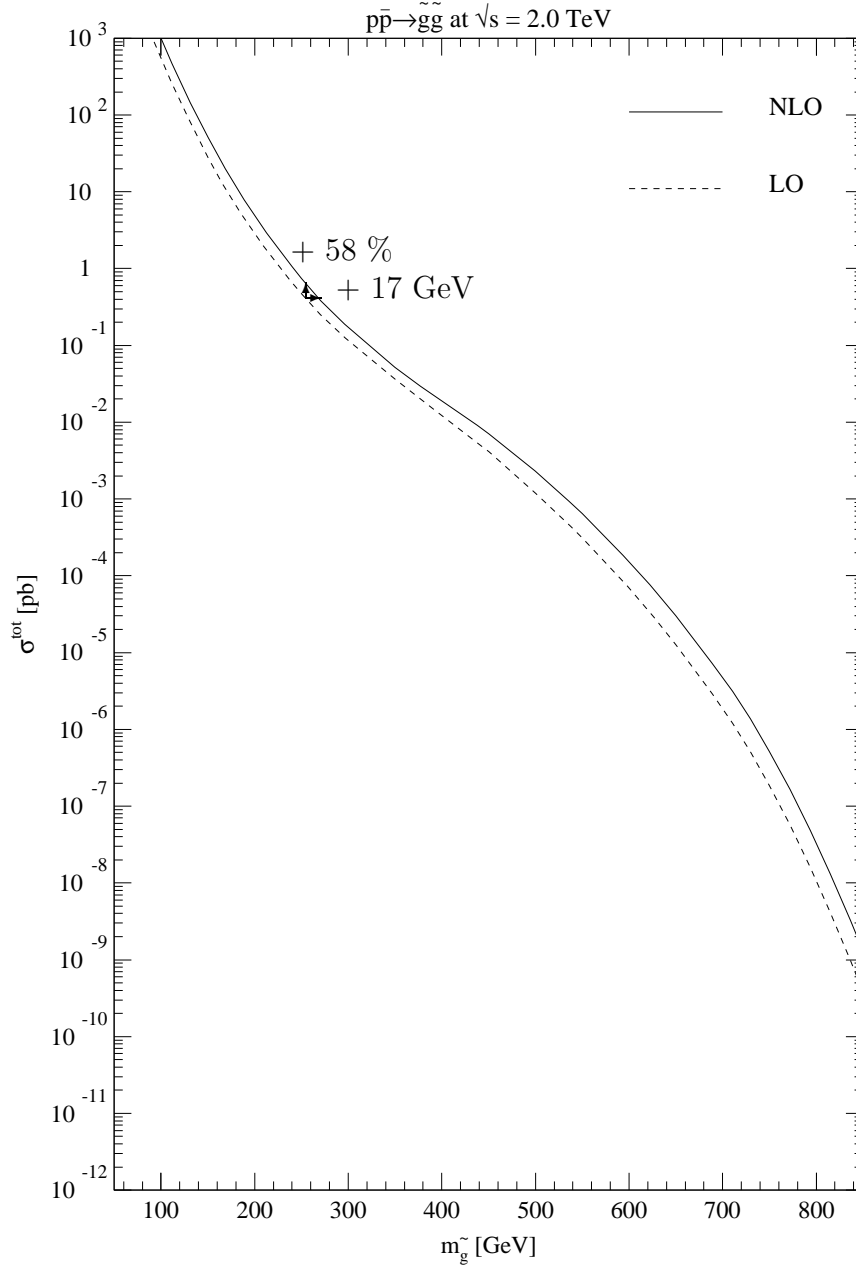


FIG. 3. Total cross section for gluino pair production at Run II of the Tevatron as a function of squark mass. The next-to-leading order cross section (full curve) exceeds the leading order cross section (dashed curve) by 58 %. Alternatively, for any measured cross section the corresponding gluino mass is shifted by 17 GeV. The squark mass has been fixed at $m_{\tilde{q}} = 250$ GeV.

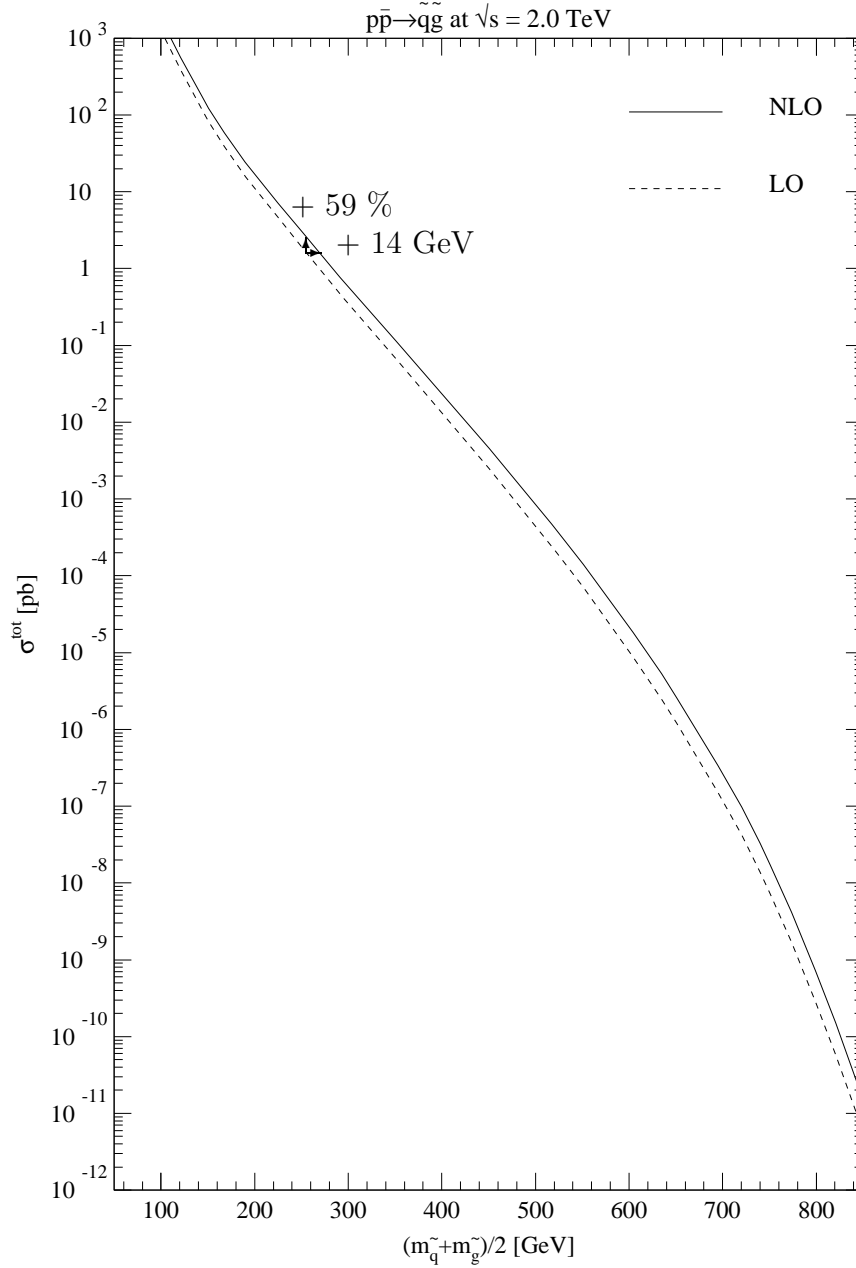


FIG. 4. Total cross section for associated production of a squark and gluino at Run II of the Tevatron as a function of the average squark and gluino mass. The next-to-leading order cross section (full curve) exceeds the leading order cross section (dashed curve) by 59 %. Alternatively, for any measured cross section the corresponding average squark and gluino mass is shifted by 14 GeV. For this plot, we have set $m_{\tilde{q}} = m_{\tilde{g}}$.

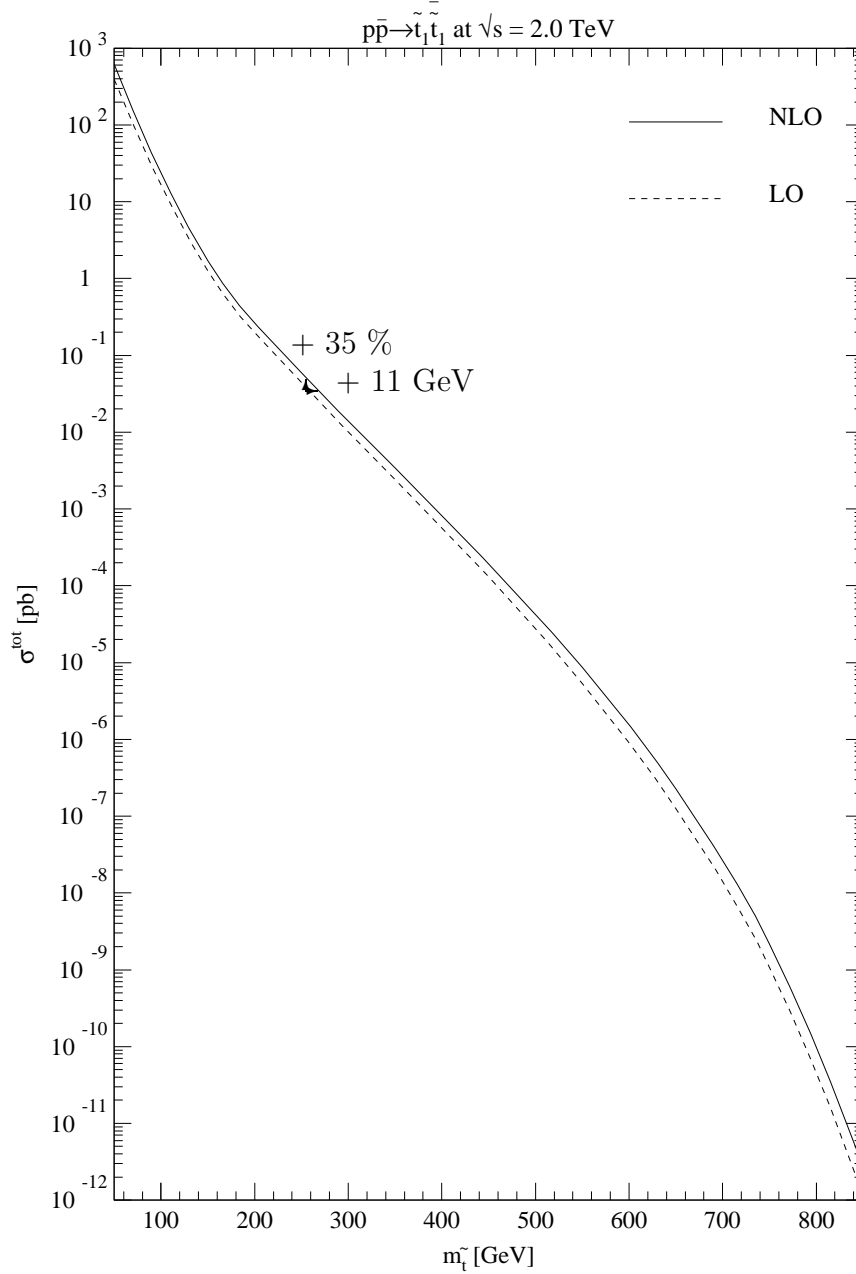


FIG. 5. Total cross section for stop-antistop production at Run II of the Tevatron as a function of the stop mass $m_{\tilde{t}_1}$. The next-to-leading order cross section (full curve) exceeds the leading order cross section (dashed curve) by 35 %. Alternatively, for any measured cross section the corresponding stop mass is shifted by 11 GeV. The light squark mass, the gluino mass, and the mixing parameter are set to $m_{\tilde{q}} = 256$ GeV, $m_{\tilde{g}} = 284$ GeV, and $\sin(2\tilde{\theta}) = -0.99$.

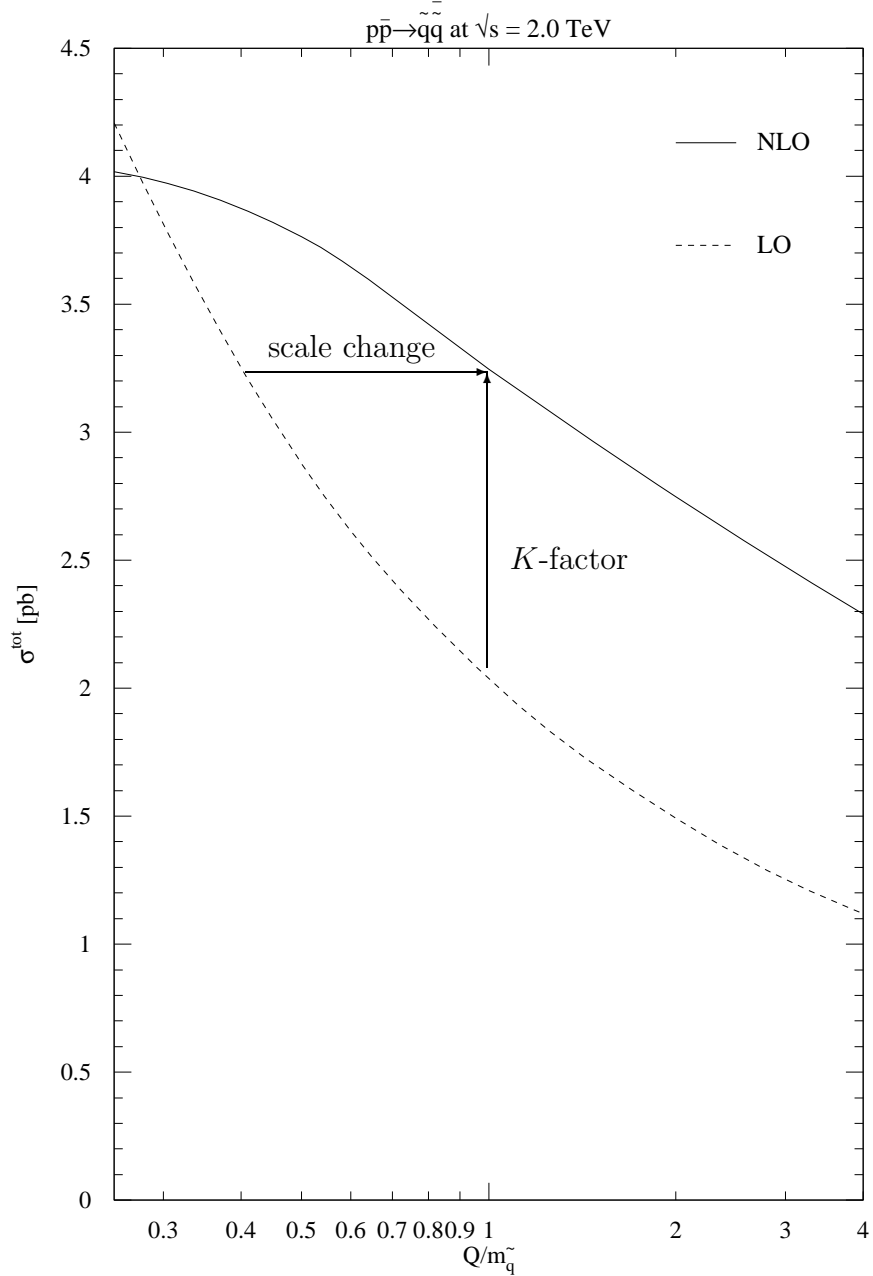


FIG. 6. Total cross section for squark-antisquark production at Run II of the Tevatron as a function of the common renormalization and factorization scale Q . The squark mass has been fixed at $m_{\tilde{q}} = 250$ GeV, and $m_{\tilde{g}} = 250$ GeV. For $Q = m_{\tilde{q}}$, the next-to-leading order cross section (full curve) can be obtained from the leading order cross section (dashed curve) if the latter is multiplied by a K -factor of 1.59. The same result is obtained if a hard scale of $Q = 0.41 m_{\tilde{q}}$ is used in the calculation of the leading order cross section.

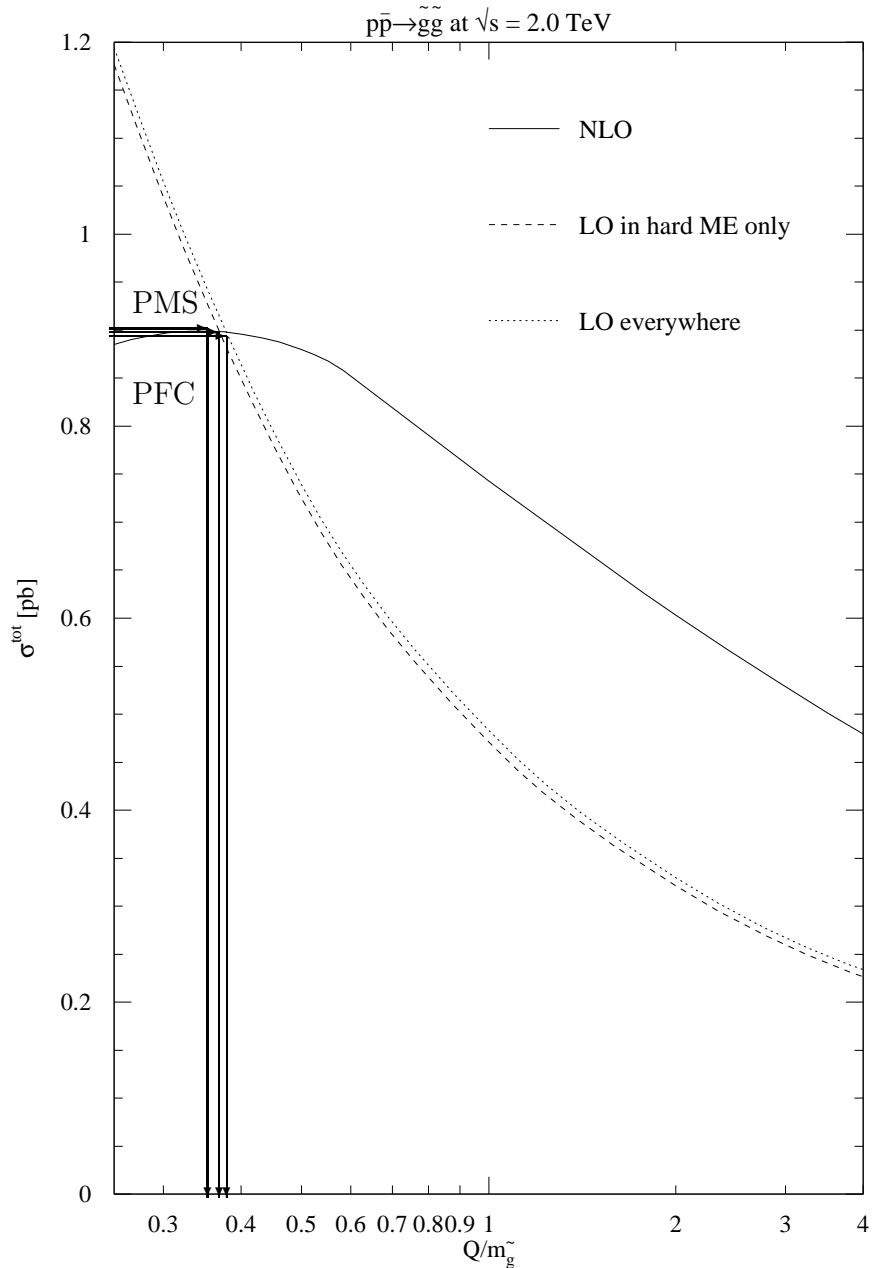


FIG. 7. Total cross section for gluino pair production at Run II of the Tevatron as a function of the common renormalization and factorization scale Q . The gluino mass has been fixed at $m_{\tilde{g}} = 250$ GeV, and $m_{\tilde{q}} = 250$ GeV. The scales preferred by the Principle of Minimal Sensitivity (PMS, $Q = 0.35 m_{\tilde{g}}$) and the Principle of Fastest Convergence (PFC, $Q = 0.36 m_{\tilde{g}}$) are close to each other if the use of leading order expressions is restricted to the hard matrix element. If the parton densities and α_s are calculated in leading order as well, the PFC scale shifts to $Q = 0.37 m_{\tilde{g}}$.

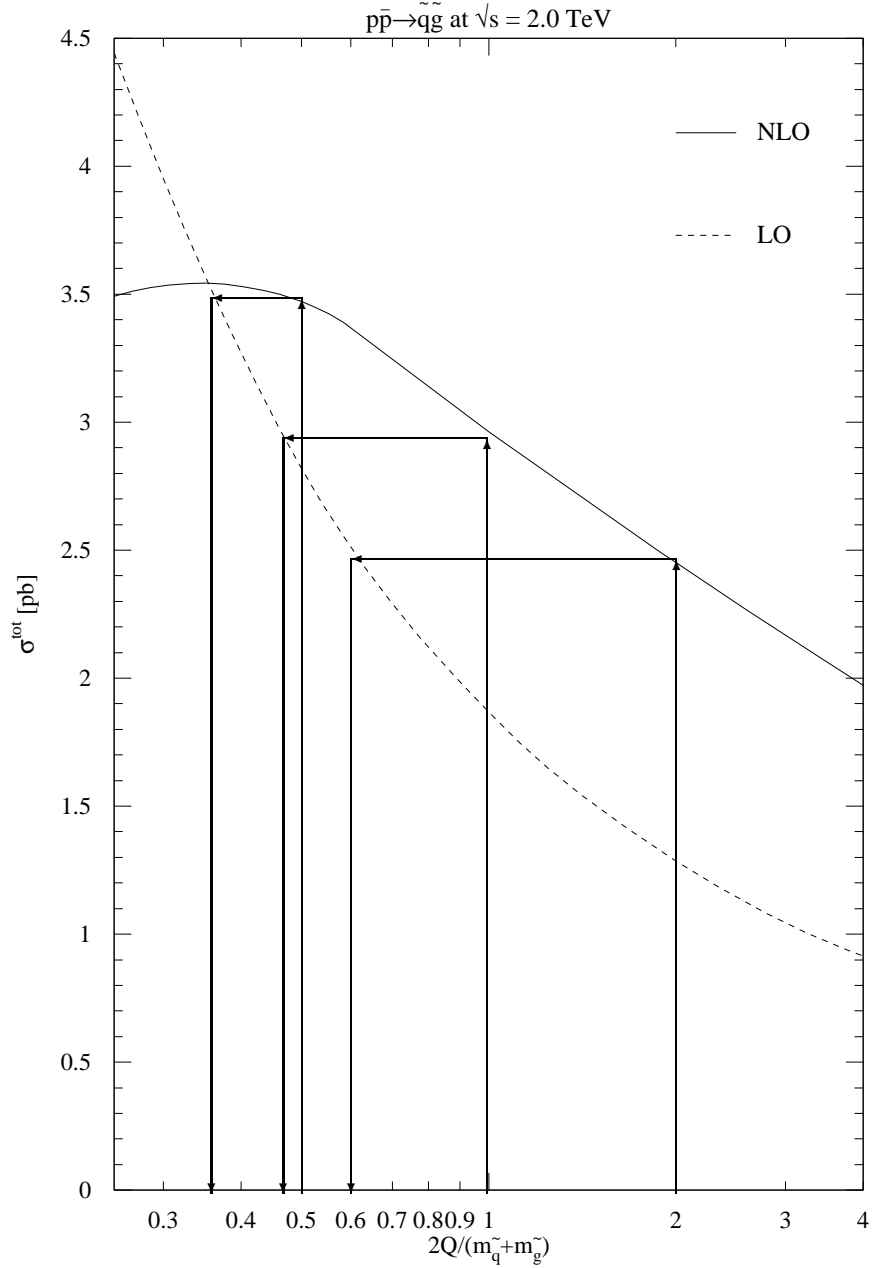


FIG. 8. Total cross section for associated production of a squark and gluino at Run II of the Tevatron as a function of the common renormalization and factorization scale Q . The squark and gluino masses have been fixed at $m_{\tilde{q}} = m_{\tilde{g}} = 250$ GeV. The three different scale choices of $2Q_{\text{NLO}}/(m_{\tilde{q}} + m_{\tilde{g}}) = [0.5; 1.0; 2.0]$ define the theoretical uncertainty at next-to-leading order. The corresponding cross sections are reproduced in leading order by $2Q_{\text{LO}}/(m_{\tilde{q}} + m_{\tilde{g}}) = [0.35; 0.475; 0.6]$.

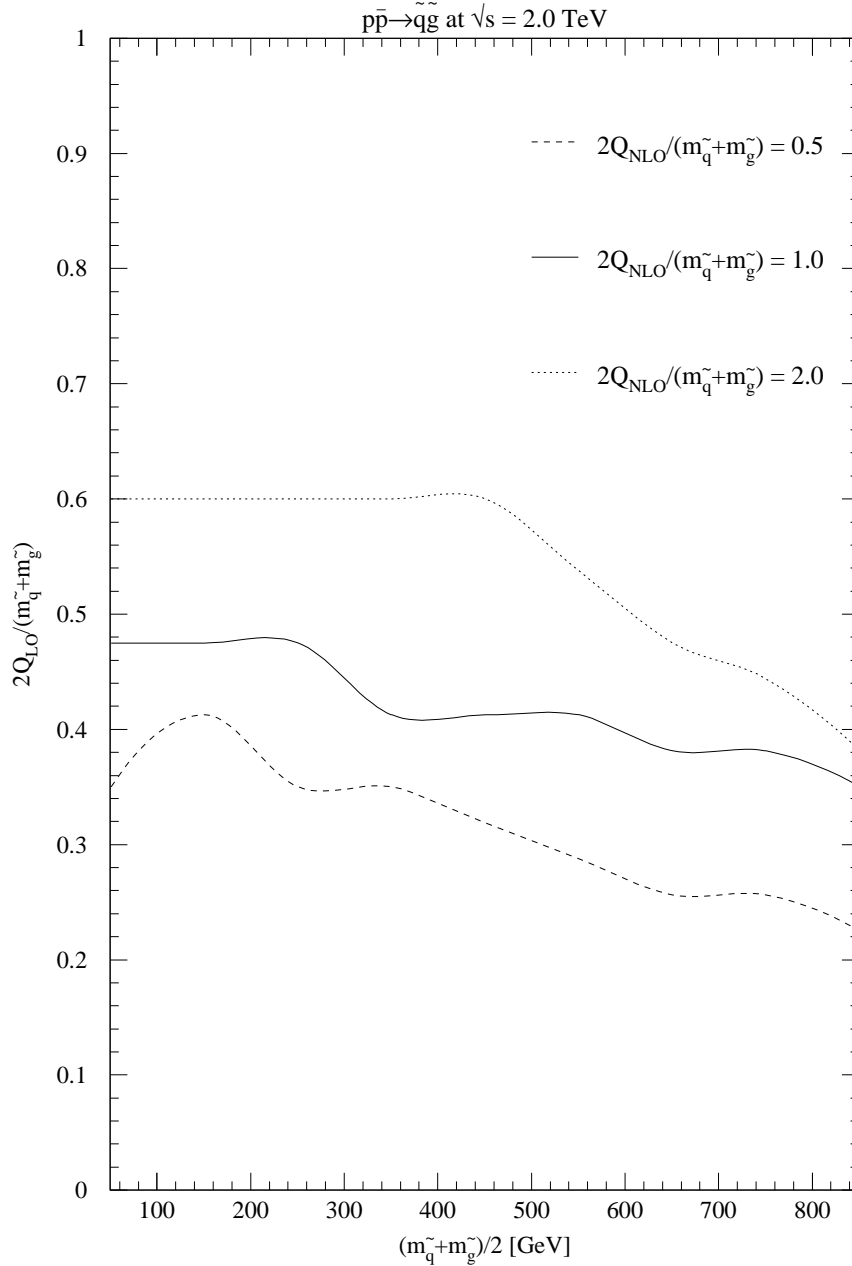


FIG. 9. Optimal scale choices for associated production of a squark and gluino at Run II of the Tevatron as a function of the average squark and gluino mass $(m_{\tilde{q}} + m_{\tilde{g}})/2$. For the central (full) curve, the NLO scale has been chosen equal to the average squark and gluino mass. The dashed and dotted curves correspond to the remaining uncertainty at NLO from a variation of $2Q_{\text{NLO}}/(m_{\tilde{q}} + m_{\tilde{g}}) = [0.5; 2.0]$. For this plot, we have set $m_{\tilde{q}} = m_{\tilde{g}}$.

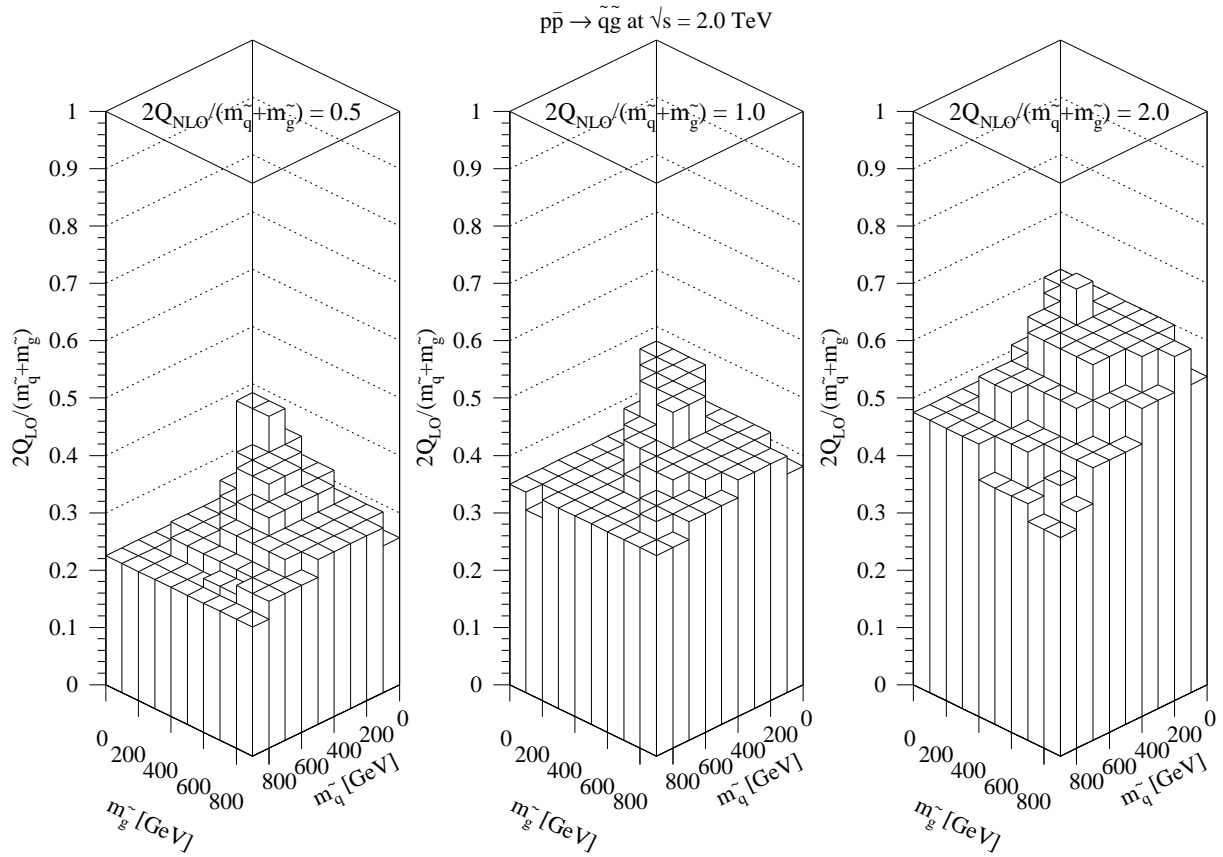


FIG. 10. Optimal scale choices for associated production of a squark and gluino at Run II of the Tevatron as a function of the squark mass $m_{\tilde{q}}$ and the gluino mass $m_{\tilde{g}}$ for three different choices of $2Q_{\text{NLO}}/(m_{\tilde{q}} + m_{\tilde{g}}) = [0.5(\text{left}); 1.0(\text{middle}); 2.0(\text{right})]$. The dependence on $m_{\tilde{q}}$ and $m_{\tilde{g}}$ separately is much weaker than along the diagonal representing the average squark and gluino mass $(m_{\tilde{q}} + m_{\tilde{g}})/2$ that sets the correct scale for the process.

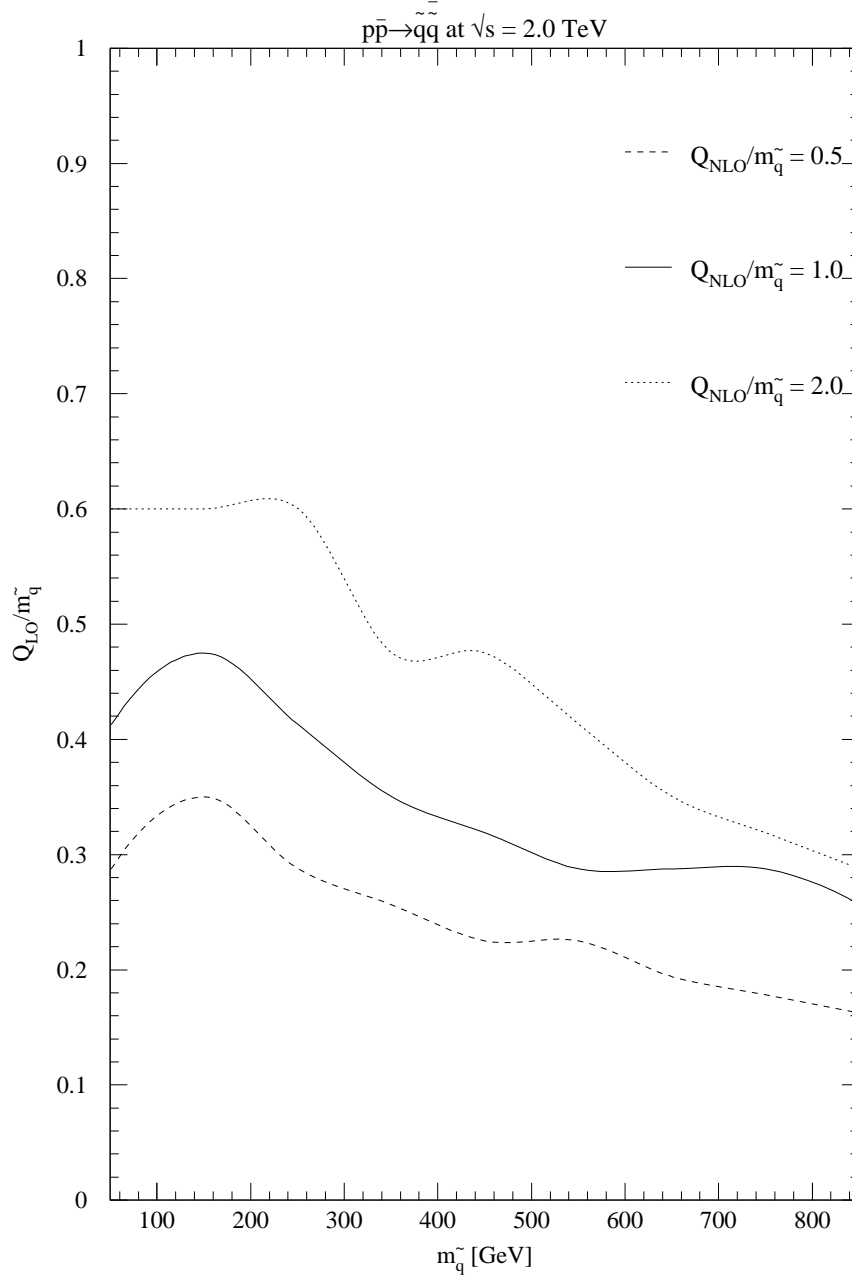


FIG. 11. Optimal scale choices for squark-antisquark production at Run II of the Tevatron as a function of the squark mass $m_{\tilde{q}}$ with $m_{\tilde{q}} = 250$ GeV. For the central (full) curve, the NLO scale has been chosen equal to the squark mass. The dashed and dotted curves correspond to the remaining uncertainty at NLO from a variation of $Q_{\text{NLO}}/m_{\tilde{q}} = [0.5; 2.0]$.

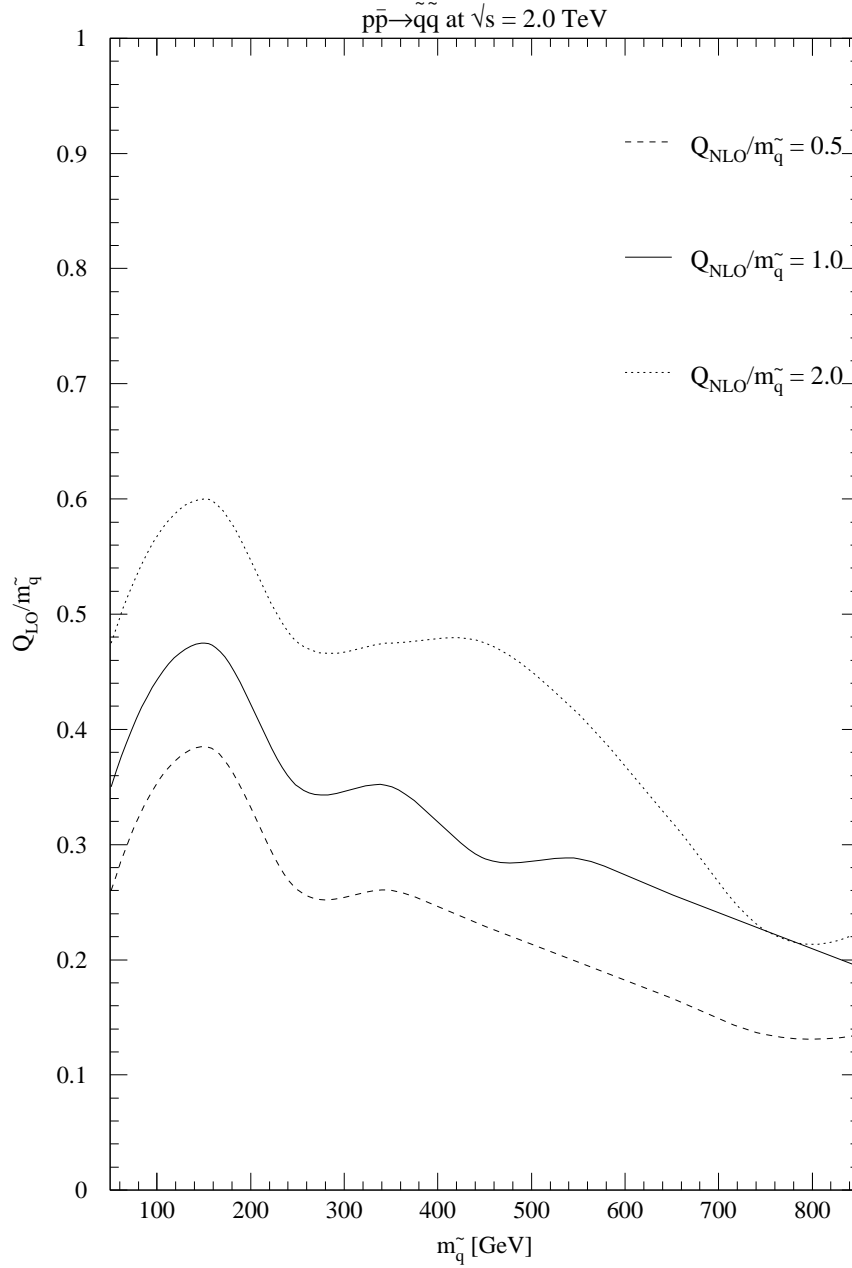


FIG. 12. Optimal scale choices for squark pair production at Run II of the Tevatron as a function of the squark mass $m_{\tilde{q}}$ with $m_{\tilde{g}} = 250$ GeV. For the central (full) curve, the NLO scale has been chosen equal to the squark mass. The dashed and dotted curves correspond to the remaining uncertainty at NLO from a variation of $Q_{\text{NLO}}/m_{\tilde{q}} = [0.5; 2.0]$.

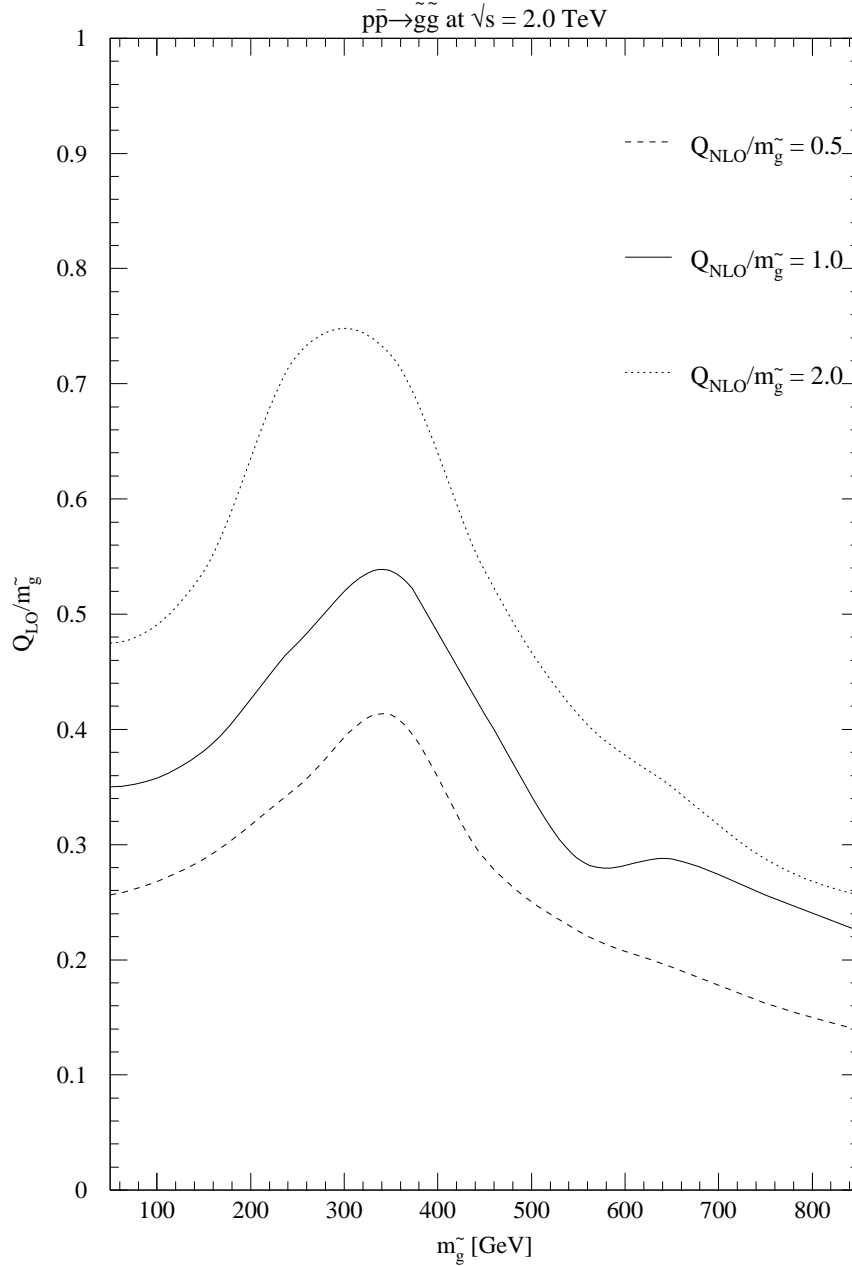


FIG. 13. Optimal scale choices for gluino pair production at Run II of the Tevatron as a function of the gluino mass $m_{\tilde{g}}$ with the squark mass fixed at $m_{\tilde{q}} = 250$ GeV. For the central (full) curve, the NLO scale has been chosen equal to the gluino mass. The dashed and dotted curves correspond to the remaining uncertainty at NLO from a variation of $Q_{\text{NLO}}/m_{\tilde{g}} = [0.5; 2.0]$. The optimal scale shows a large sensitivity in the region where $m_{\tilde{g}} = m_{\tilde{q}} = 250$ GeV.

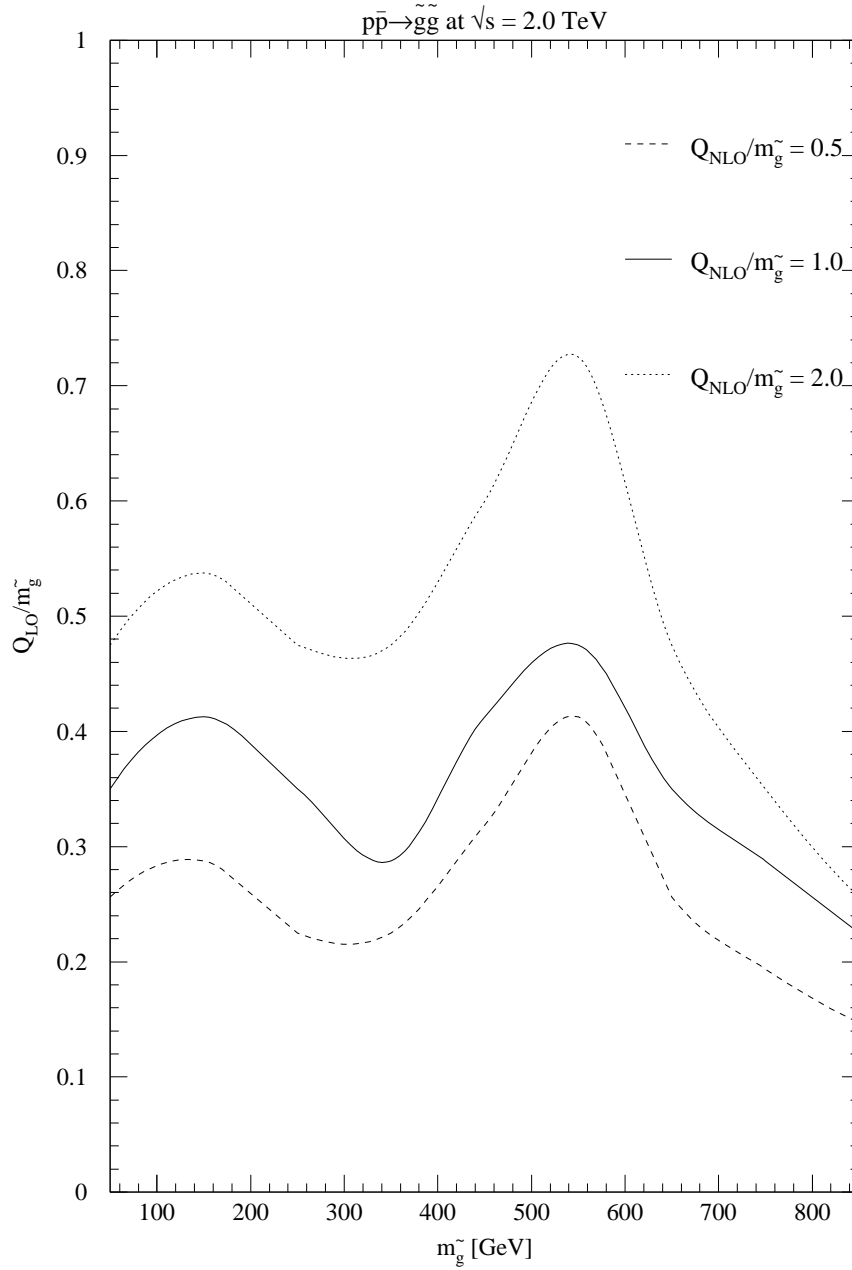


FIG. 14. Same as Fig. 13 for a squark mass of $m_{\tilde{q}} = 450$ GeV.

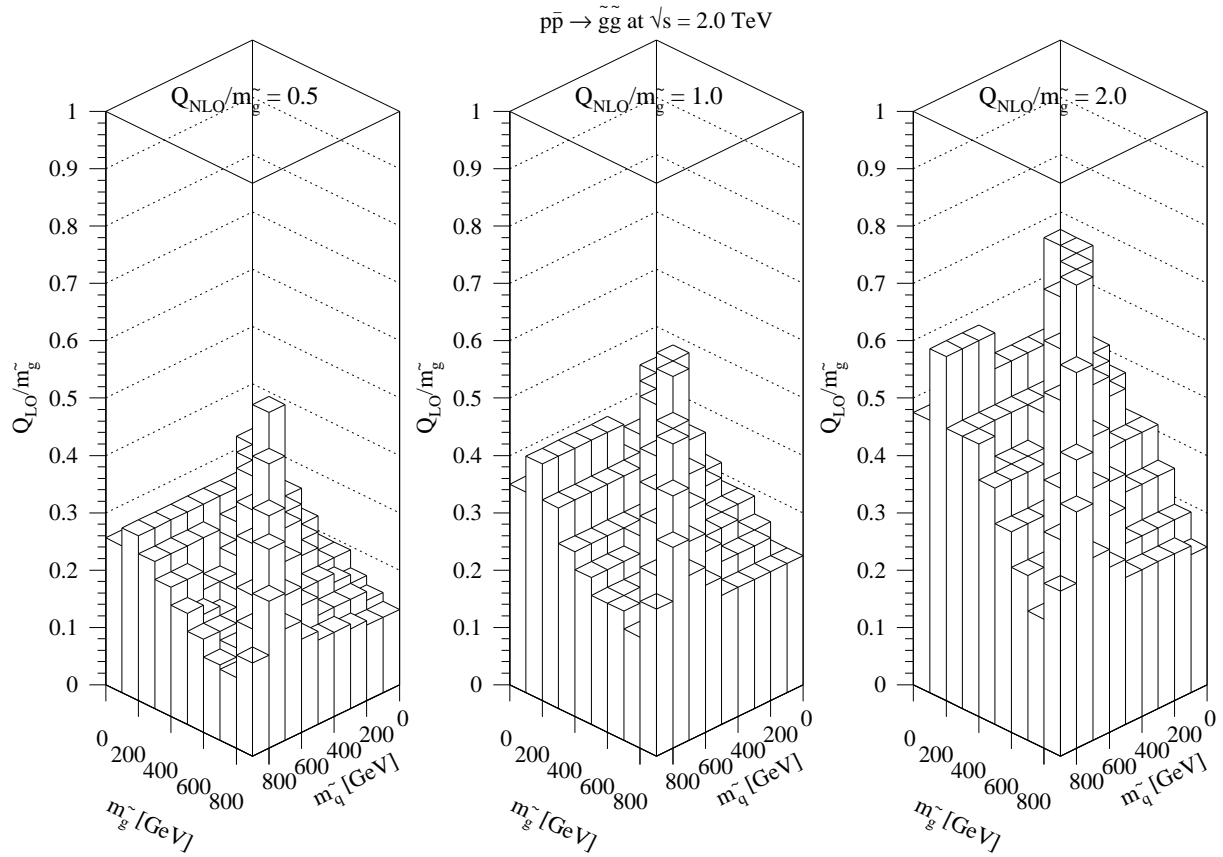


FIG. 15. Optimal scale choices for gluino pair production at Run II of the Tevatron as a function of the gluino mass $m_{\tilde{g}}$ and the squark mass $m_{\tilde{q}}$ for three different choices of $Q_{NLO}/m_{\tilde{g}} = [0.5(\text{left});1.0(\text{middle});2.0(\text{right})]$. The optimal scale shows a large sensitivity along the diagonal where $m_{\tilde{g}} = m_{\tilde{q}}$.

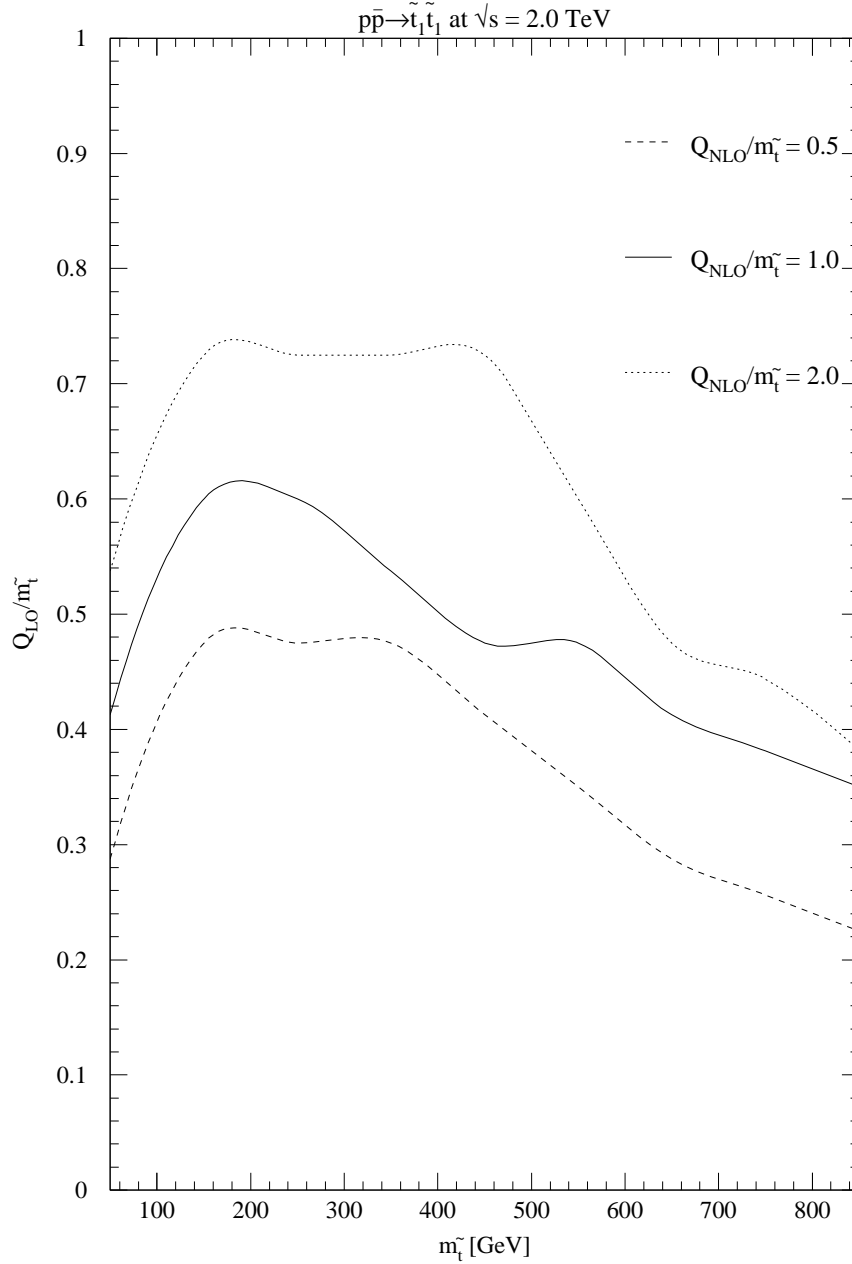


FIG. 16. Optimal scale choices for stop-antistop production at Run II of the Tevatron as a function of the stop mass $m_{\tilde{t}_1}$. For the central (full) curve, the NLO scale has been chosen equal to the stop mass. The dashed and dotted curves correspond to the remaining uncertainty at NLO from a variation of $Q_{\text{NLO}}/m_{\tilde{t}_1} = [0.5; 2.0]$. The light squark mass, gluino mass, and mixing parameter are the same as in Fig. 5.